Experimental and numerical studies on the load-carrying capacity of notched concrete beams

Z. Shi, M. Nakano, and K. Yamakawa
R&D Center, Nippon Koei Co., Ltd., Japan

ABSTRACT: This experimental investigation focuses on the maximum loads of notched concrete beams under four-point bending and the corresponding failure modes. The fracture process involving multiple cracks is also analyzed using the extended fictitious crack model. It is clearly demonstrated that the change of cracking behavior and failure mode may lead to a significant reduction in the load-carrying capacity of the simple beam. The mechanism of the phenomenon is explained, and its engineering implication is discussed.

1 INTRODUCTION

In a recent numerical study of the load-carrying capacity of notched concrete beams, a strong dependence of the maximum load on the failure mode was revealed (Shi & Suzuki 2004). The loading conditions and notch arrangements of the simple beams in the original study are illustrated in Figure 1. As shown, among the three notches introduced into the beam notches, A and B were kept at a constant size of 10 mm while notch C was assigned various sizes to study the relations between the maximum loads and failure modes under eccentric loading. The obtained relations are shown in Figure 2, which contains two curves. When the eccentric load was applied at notch C, a monotonically decreasing relation between the peak load and the size of notch C was obtained, and the dominating crack for beam failure was shown to invariably develop from notch C. On the other hand, when the eccentric load was applied at notch A, the obtained maximum load seemed to be unaffected by the enlargement of notch C until it reached a critical value, beyond which the peak load decreased quickly as the size of notch C increased. It was shown that two failure modes were involved in the latter case. Before reaching the threshold value of notch C, the dominating crack for the beam failure originated from notch A; beyond that point it developed from notch C.

The purpose of this study was to provide experimental evidence for the strong dependence of the load-carrying capacity of a structural member on the failure mode. The experimental investigation focuses on the maximum loads of notched concrete beams under four-point bending and the corresponding failure modes. The fracture processes involving multiple cracks are also analyzed using the extended fictitious crack model, which has been employed successfully to analyze multiple discrete cracks in concrete (Shi et al., 2001, 2003, 2004; Shi 2004). The mechanism of the phenomenon is explained, and its engineering implication is discussed.

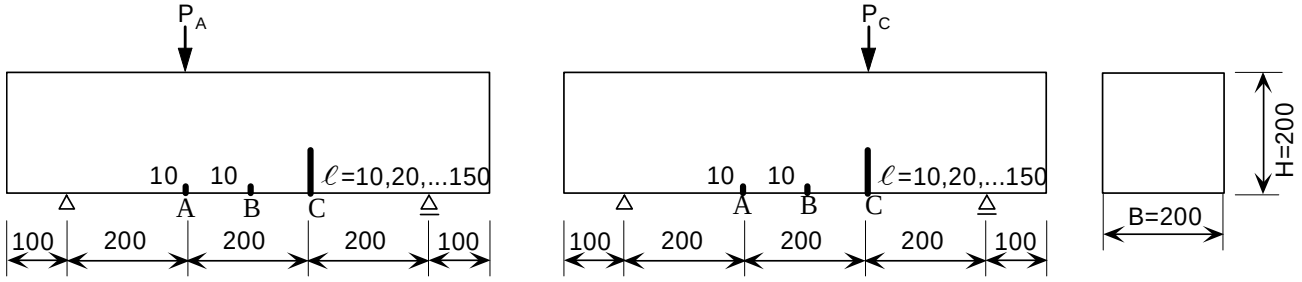

Dimensions in mm

Case 2-3 Case 2-4

Figure 1. Numerical models of eccentric loading tests (Shi & Suzuki 2004)

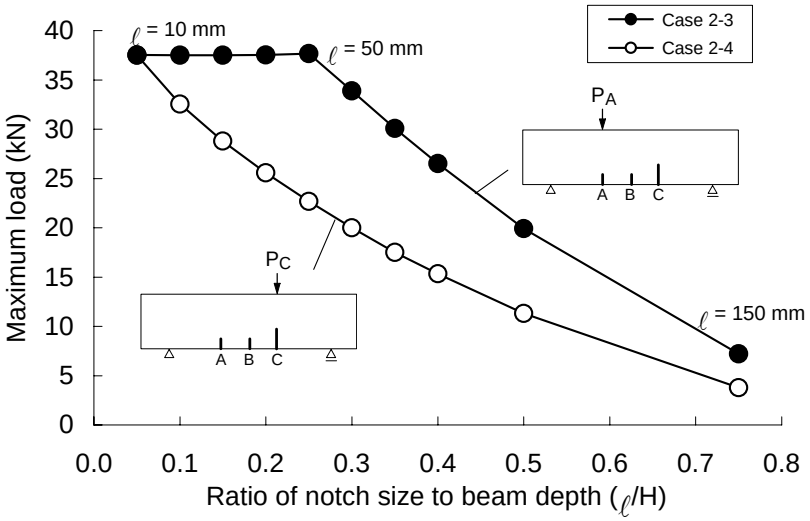

Figure 2. Relations between maximum load and ratio of notch size to beam depth (Shi & Suzuki 2004)

2 FOUR-POINT BENDING TESTS

The four-point bending tests and geometric details of the specimens are illustrated in Figure 3. Three small notches of the same size of 10 mm were introduced into plain concrete beams, located directly below the two loading points and at the midspan, respectively. Then a fourth notch was introduced into the same specimens, which varied in size and served as a control notch for switching the failure mode to demonstrate the transition of fracture processes in the beam at a critical notch size. The mix proportions of concrete are summarized in Table 1, and the material properties of the test specimens are given in Table 2. Table 3 shows the test cases and notch arrangements. As seen, five cases were tested with the size of notch D changing from 0 to 100 mm, and for each case three specimens were prepared.

The results of the tests are summarized in Table 4, which includes the maximum load and the location of the failure cross section. Photos of the failed beams are shown in Figure 4. With only three notches in case 1, two specimens failed at notch B and one broke at notch C. By introducing an additional notch of 30 mm into the beam in case 2, the three specimens all failed at notch B. The results suggest that notch D replaced notches A and C as a new stress concentration point for potentially active cracks to emerge and to compete with cracks from

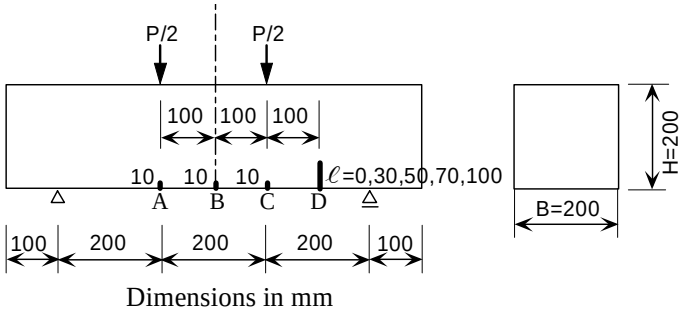

Dimensions in mm

Figure 3. Four-point bending test

Table 1. Concrete composition

Maximum size of coarse aggregate (mm)	Slump (cm)	Air (%)	W/C ratio (%)	Sand-coarse aggregate ratio (%)	Unit weight (kg/m^3)					
					Water W	Cement C	Fine aggregate S	Coarse aggregate G	Admixture	
									AE_1	AE_2
15	12.5	4.8	60.0	50.0	170	283	898	926	250ml/ C=100kg	C× 0.0005

Note: AE_1 = Air-entraining and water-reducing agent

AE_2 = Air-entraining agent

Table 2. Material properties of concrete

Material prop. / Curing period	Compressive strength (N/mm^2)		Modulus of elasticity (kN/mm^2)		Tensile strength (N/mm^2)	
	Individual specimen	Average	Individual specimen	Average	Individual specimen	Average
Cured for 7 days	23.68	23.21	24.43	23.83	2.68	2.42
	22.66		24.06		2.15	
	23.30		22.99		2.44	
Cured for 28 days	35.91	36.80	25.72	26.06	3.06	2.82
	39.22		27.16		2.41	
	35.27		25.30		2.98	

Table 3. Test cases and notch arrangements

Test case	Notch size (mm)				Number of specimens
	A	B	C	D	
Case 1	10	10	10	0	3
Case 2	10	10	10	30	3
Case 3	10	10	10	50	3
Case 4	10	10	10	70	3
Case 5	10	10	10	100	3

notch B. In case 3 one specimen broke at notch D and two others failed at notch B, indicating that at 50 mm notch D may have approached its threshold value for the failure mode to change. For cases 4 and 5 all specimens failed at notch D, and their maximum loads were much lower. Based on these experimental observations, it is concluded that notch D indeed served as a control notch for altering failure modes, and thus providing an effective way to investigate the relations between failure modes and the load-carrying capacity of a structural member.

Table 4. Results of fracture tests

Test case	Specimen No.	Maximum load (kN)		Location of fracture
		Individual specimen	Average	
Case 1	1	50.0	48.8	Notch B
	2	50.6		Notch C
	3	45.7		Notch B
Case 2	1	43.0	44.7	Notch B
	2	46.8		Notch B
	3	44.2		Notch B
Case 3	1	44.7	43.1	Notch D
	2	38.4		Notch B
	3	46.2		Notch B
Case 4	1	36.0	32.7	Notch D
	2	32.2		Notch D
	3	29.8		Notch D
Case 5	1	22.2	21.6	Notch D
	2	21.8		Notch D
	3	20.8		Notch D

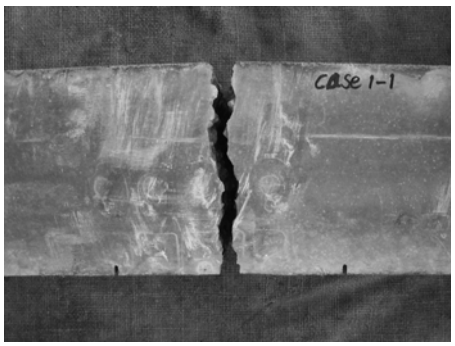

Case 1-1

Case 2-1

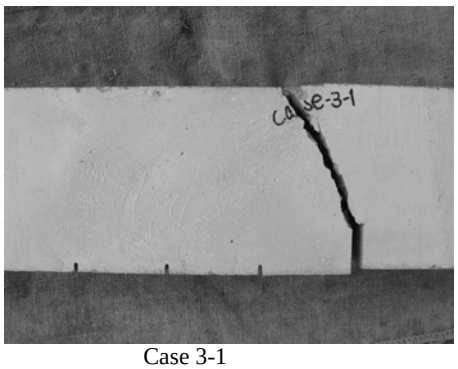

Case 3-1

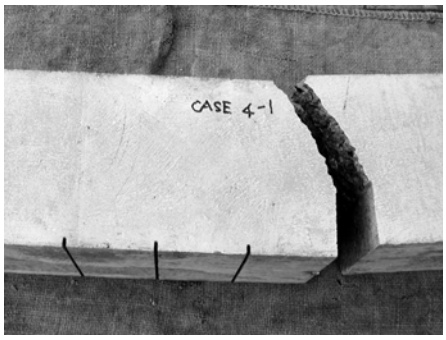

Case 4-1

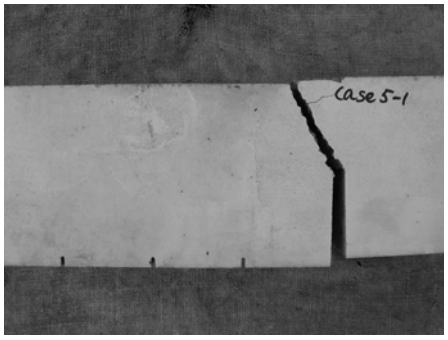

Case 5-1

Figure 4. Locations of the failure cross-sections

3 NUMERICAL ANALYSES

In the following, crack analyses of the mode I type are carried out using the extended fictitious crack model. The FE mesh is illustrated in Figure 5, where the size of notch D is assigned values from 0 to 150 mm with an increment of 10 mm. As seen, the mesh size in the vertical direction is set to 10 mm, which is one twentieth of the beam height. According to the preliminary study on mesh-size sensitivity, as the mesh size was changed from 10 mm to 5 mm, the maximum loads decreased slightly and the range of variation was within 3%. In order to solve the crack equations (Shi et al. 2001), the bi-linear tension softening relation as shown in Figure 6 is employed (Rokugo et al. 1989). The material properties for numerical studies are summarized in Table 5, which includes the elastic modulus E, the tensile strength f_t, the compressive strength f_c, Poisson's ratio υ, and the estimated fracture energy G_F.

The obtained analytical relations between the peak load and the ratio of notch size (notch D) to beam depth are shown in Figure 7, and the crack propagation charts are illustrated in Figure 8. Note that in Figure 8 the circled numbers along the crack path denote the tip position of that particular crack at the designated step of the crack-tip-controlled computation. Also shown in Figure 7 are the test results that are considered to verify the numerical predictions except for case 1, in which notch D was not yet introduced into the beam and higher peak loads were observed in the three tests. Compared with the average value of the test results the discrepancy is 12%, which may have been caused by the inaccuracy in the notch processing and inherent variations in the materials. As seen, numerical analyses predict that the peak load of the beam will not be affected by the introduction of notch D when its size is less than 50 mm, and that the beam will break at the midspan (Fig. 8). However, as notch D reaches 50 mm, completely different cracking behavior emerges and the beam fails at notch D. A careful examination of the crack propagation charts reveals competition between crack B and crack D before the latter finally dominates the failure process in the postpeak regions. As the size of notch D exceeds 50 mm, cracking behaviors exhibit little change and the beam

Table 5. Material properties for numerical studies

E (kN/mm^2)	ν	f_c (N/mm^2)	f_t (N/mm^2)	G_F (N/mm)
26.1	0.2	36.8	2.8	0.1

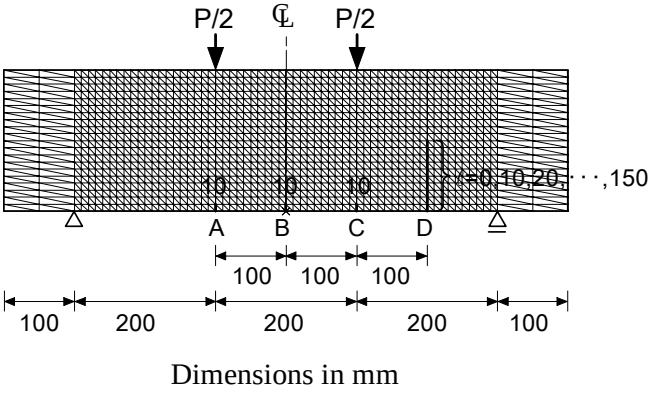

Figure 5. FE mesh of four-point bending tests

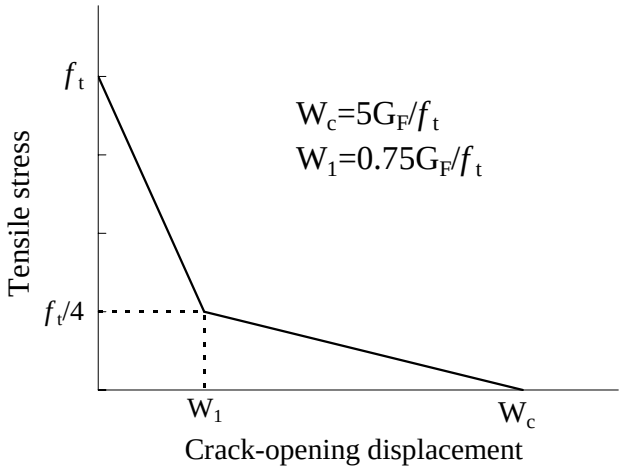

Figure 6. Bilinear tension-softening relation of concrete

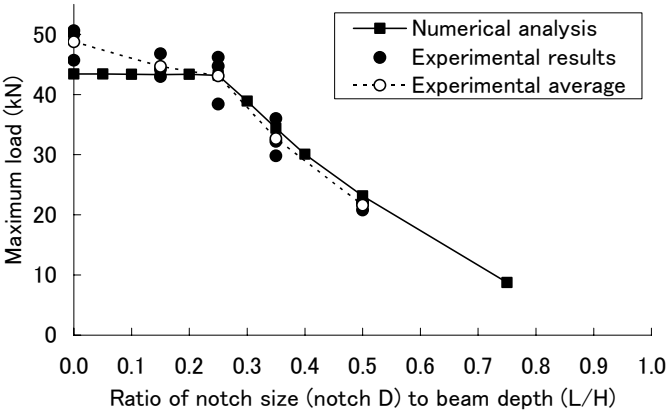

Figure 7. Relations between maximum load and ratio of notch size to beam depth

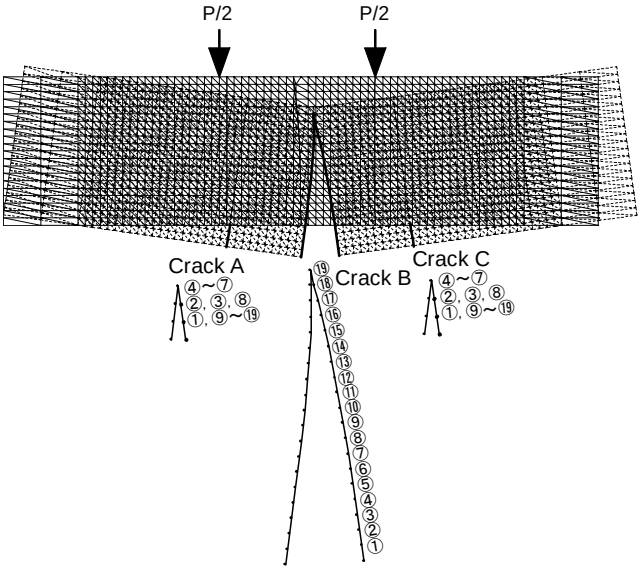

Notch D = 0 mm (Test case 1)

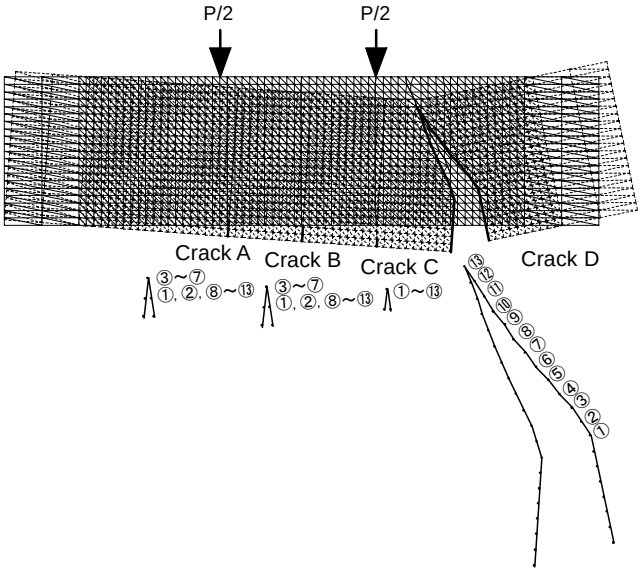

Notch D = 70 mm (Test case 4)

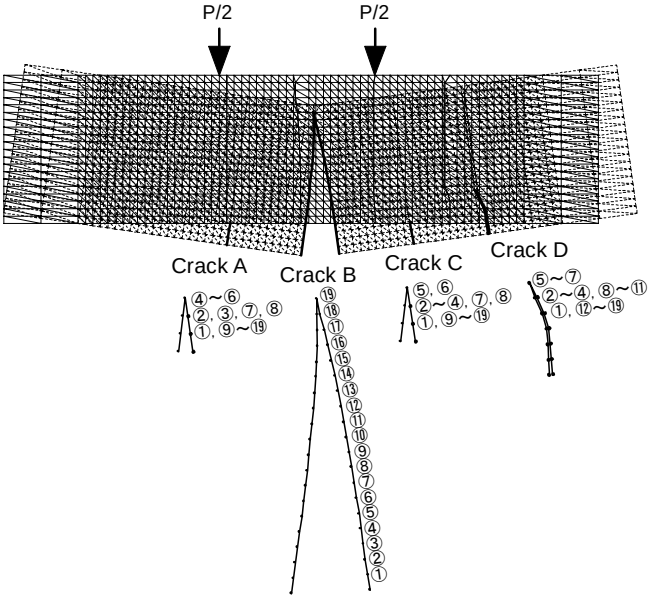

Notch D = 30 mm (Test case 2)

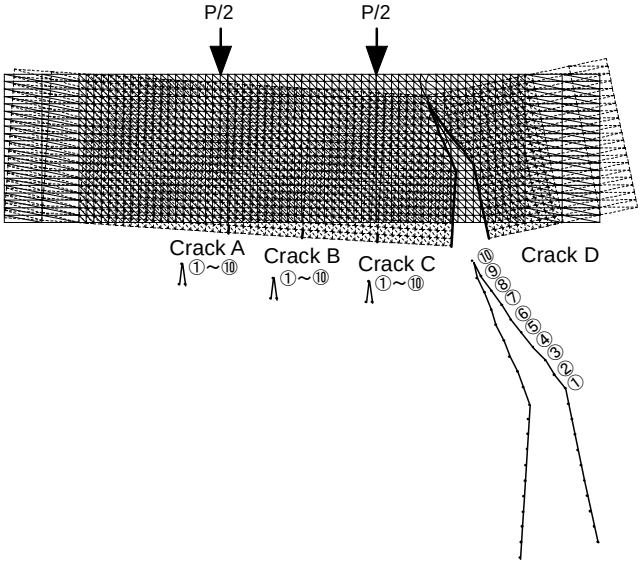

Notch D = 100 mm (Test case 5)

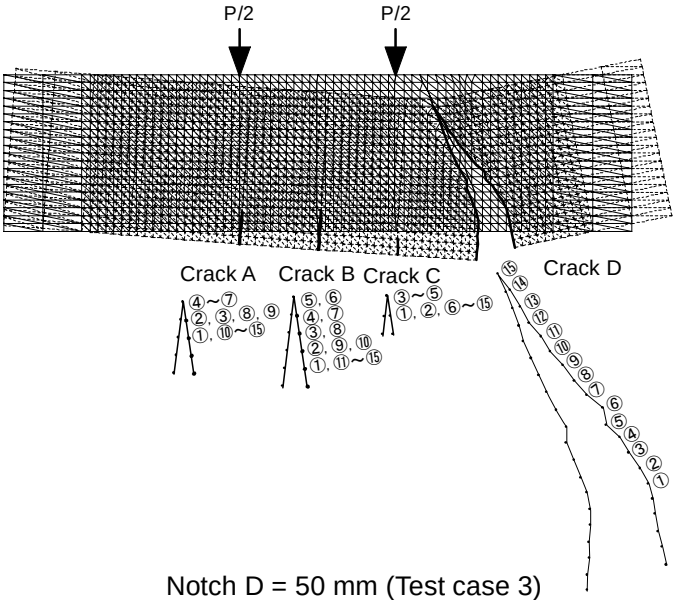

Notch D = 50 mm (Test case 3)

Figure 8. Crack propagation charts

always breaks at notch D. Obviously, the most important characteristic of the beam with the change of failure mode is the significant decrease in its load-carrying capacity (due to the reduction of the effective cross section at notch D), as shown in Figure 7.

For reference, the analytical and experimental relations between load and midspan displacement are presented in Figure 9, and the load-CMOD relations at notch D are illustrated in Figure 10. Note that during the tests, data was recorded up to the peak load only.

4 ENGINEERING IMPLICATION AND CONCLUSION

As clearly revealed by the present study, the change of cracking behavior and failure mode may result in a significant reduction of the load-carrying capacity of the simple beam. This fact may have significant implications in clarifying the fatigue mechanisms of certain engineering materials.

In studies of metal fatigue, it has long been known that the fatigue strength of a test specimen is

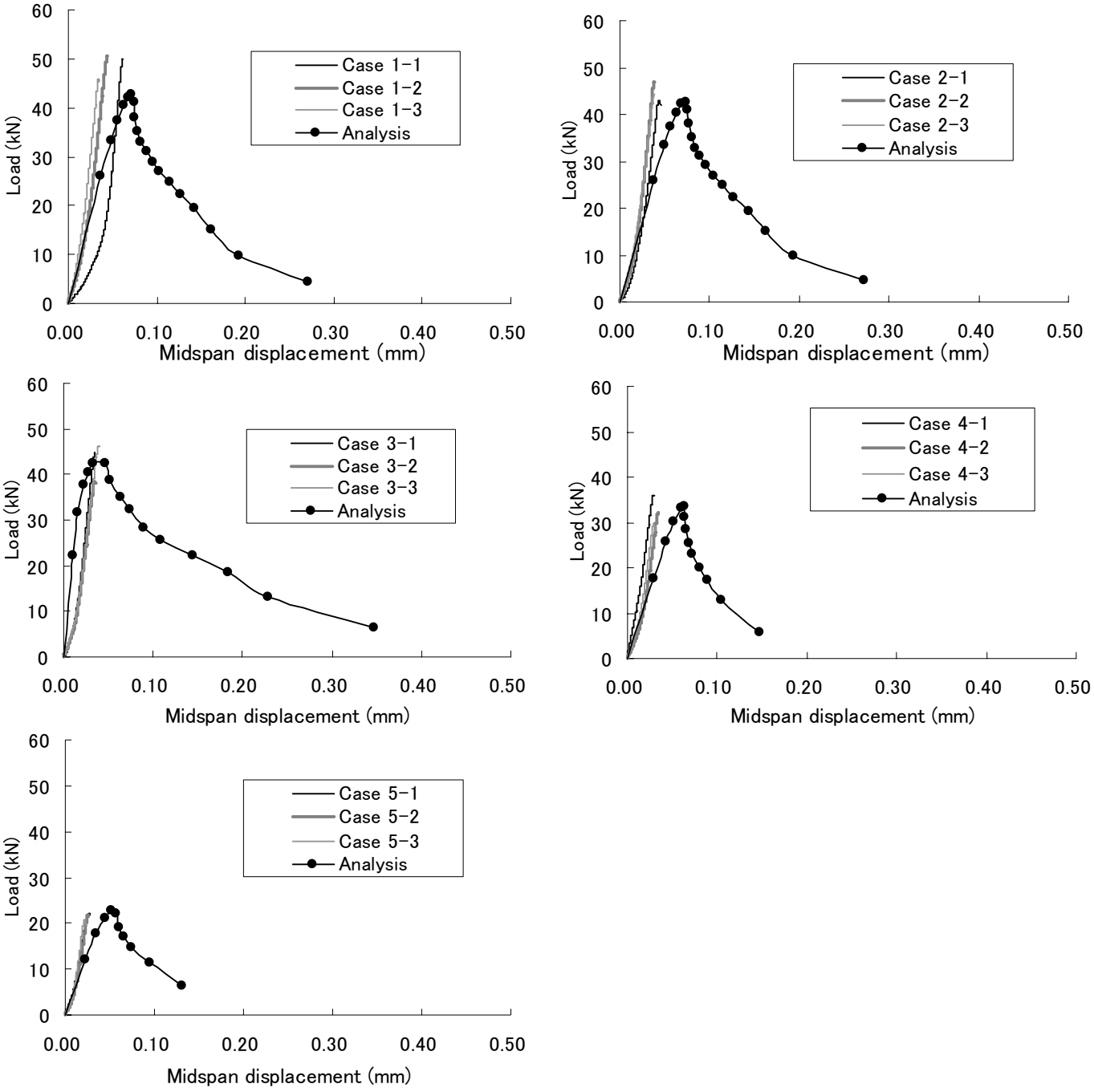

Figure 9. Load - midspan displacement relations

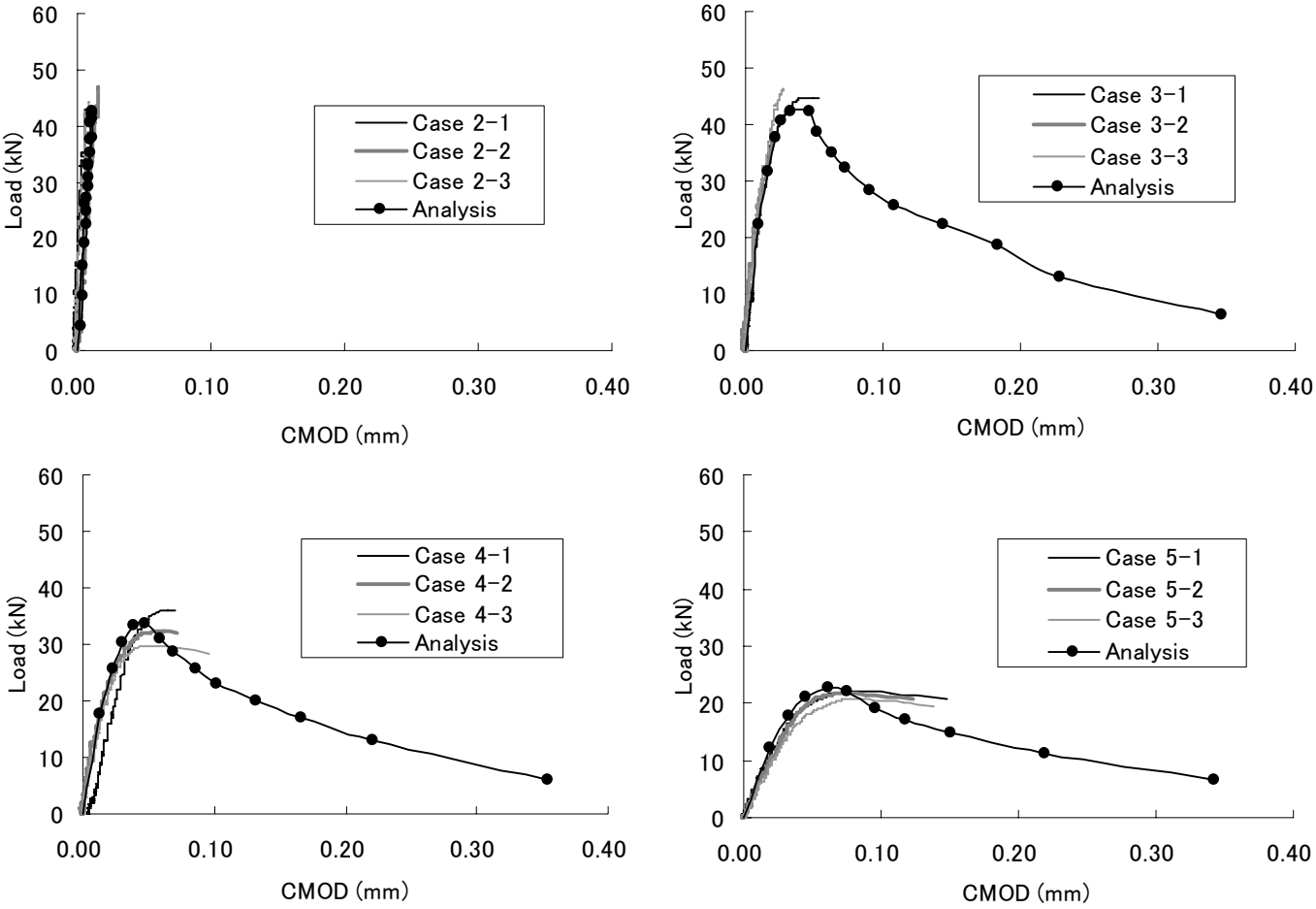

Figure 10. Load - CMOD relations at notch D

not affected by introducing artificial micro cavities into the specimen unless the size of these artificial defects exceeds a critical value, beyond which a significant reduction in fatigue strength takes place (Murakami 1993). In general, initial defects exist in all structural members; only the degree of imperfection varies. Under actual cyclic loading, not only the amplitude but also the loading position may change. Eventually, the material weakening process of a structural member caused by repeated loading inevitably involves multiple cracking activities and multiple cracking behaviors appear depending on specific loading stages. As a threshold value in terms of a critical crack length or a critical crack density (such as the maximum number of cracks in a certain location), etc., is approached, unexpected cracking behaviors may abruptly emerge and replace the previous ones, thus leading to a new type of material failure with a much smaller load-carrying capacity.

REFERENCES

Murakami, Y. 1993. *Metal fatigue: Effects of small defects and nonmetallic inclusions*: 33-53.Tokyo: Yokendo.

Rokugo, K., Iwasa, M., Suzuki, T., Koyanagi, W. 1989. Testing methods to determine tensile strain softening curve and fracture energy of concrete. In: H. Mihashi, H. Takahashi, F.H. Wittmann (eds), *Fracture toughness and fracture energy - test method for concrete and rock*: 153-163. Rotterdam: Balkema.

Shi, Z. 2004. Numerical analysis of mixed-mode fracture in concrete using extended fictitious crack model. *Journal of Structural Engineering* 130(11): 1738-1747.

Shi, Z. & Suzuki, M. 2004. Numerical studies on load-carrying capacities of notched concrete beams subjected to various concentrated loads. *Construction and Building Materials* 18: 173-180.

Shi, Z., Suzuki, M., Nakano, M. 2003. Numerical analysis of multiple discrete cracks in concrete dams using extended fictitious crack model. *Journal of Structural Engineering* 129(3): 324-336.

Shi, Z., Suzuki, M., Ohtsu, M. 2004. Discrete modeling of crack interaction and localization in concrete beams with multiple cracks. *Advanced Concrete Technology*, 2(1): 101-111.

Shi, Z., Ohtsu, M., Suzuki, M., Hibino, Y. 2001. Numerical analysis of multiple cracks in concrete using the discrete approach. *Journal of Structural Engineering* 127(9): 1085-1091